Int. J. Aquat. Biol. (2025) 13(6): 60-70
ISSN: 2322-5270; P-ISSN: 2383-0956
Journal homepage: www.ij-aquaticbiology.com

Original Article

Enhanced removal of PVC nanoplastics from water using microwave-activated palm frond biochar

Zaniab J. Kadhum[1,2], Sadiq Kadhum lafta Alzurfi[*1]

[1]Department of Ecology, Faculty of Science, University of Kufa, Najaf, Iraq.
[2]Directorate of Environment in Najaf, Ministry of Environment, Najaf, Iraq.

Abstract: Nanoplastic polyvinyl chloride (PVC) is increasingly reported in aquatic environments, yet remains difficult to capture with conventional treatment. This study develops a low-cost sorbent from palm-frond waste by microwave activation and NaOH treatment, and further produces a magnetically retrievable variant by depositing Fe_3O_4. Materials prepared at 800 W for 20 min using NaOH (0.5, 2, and 4 M) were characterized by FTIR, FESEM, and XRD, then evaluated in batch tests across initial PVC concentrations of 0.2-1.0 ppm, sorbent doses of 0.1-1.0 g L^{-1}, and contact times up to 30 min. The biochar achieved complete removal at 0.2 ppm and 99% at 1.0 ppm within 30 min, with performance increasing with dose and contact time. At 0.6 ppm, removal rose from 89 to 97% as contact time approached 30 min. Spectroscopic and microscopic analyses indicate that oxygenated surface groups and hierarchical porosity underpin hydrophobic and electrostatic interactions with PVC, while magnetization enables rapid post-treatment separation without compromising the active surface. By valorizing agricultural waste into an efficient, retrievable sorbent, this work offers a practical, energy-lean pathway for nanoplastic remediation.

Article history:
Received 1 Octobe 2025
Accepted 24 November 2025
Available online 25 December 2025

Keywords:
Magnetic biochar
Microwave activation
Water treatment
Pollutant removal

Introduction

There is growing global interest in treating environmental pollutants (Lalrinfela et al., 2024), such as airborne pollutants (Fadhil et al., 2023), heavy metals, and microplastics, which pose a serious threat to human health and the ecosystem (Bashir et al., 2020; Lalrinfela et al., 2024) and stressors that further connect environmental contamination with agricultural productivity and ecosystem resilience (Fadhil et al., 2024). The challenge is particularly critical in aquatic environments, where these pollutants, alongside contaminated microorganisms (Sahira and Al-Abboodi, 2023), persist and accumulate, threatening aquatic life (Rashid et al., 2024; Salman et al., 2025).

Polyvinyl chloride (PVC) nanoplastics are particularly problematic due to their durability, small size, and ability to adsorb and transport co-pollutants through food webs (Bashir et al., 2020). In this context, biochar, a carbon-rich material produced by pyrolysis of biowaste, has emerged as a promising and cost-effective solution. It has emerged as a versatile adsorbent owing to its high surface area, hierarchical porosity, and abundant surface functional groups (Yi et al., 2018). Adsorption behavior depends strongly on feedstock chemistry and activation route, which co-determine pore architecture, surface oxygenation, and site energy distributions (He et al., 2024). Thanks to its characteristics that make it an excellent adsorbent for a wide range of pollutants (Tan et al., 2015). Several previous studies have demonstrated the effectiveness of biochar in environmental remediation. For example, magnetic biochar is highly efficient at adsorbing nano- and microplastic particles from aqueous environments (Zhang et al., 2020; Singh et al., 2021). The efficacy of biochar is significantly influenced by feedstock characteristics and activation conditions (He et al., 2024).

Microwave activation is an advantageous technique for improving biochar characteristics,

*Correspondence: Sadiq Kadhum lafta Alzurfi
E-mail: sadiqk.alzurfi@uokufa.edu.iq
DOI: https://doi.org/10.22034/ijab.v13i6.2726

offering rapid heating, uniform energy distribution, and lower energy consumption than other approaches (Paramasivan, 2022). In parallel, sustainable water-treatment strategies increasingly valorize natural and waste-derived materials (Benouis et al., 2022; Al-Saady et al., 2022). Microfluidic platforms that span acoustic streaming, chemotactic gradients, and dynamic microenvironments provide high-precision tools for probing particle-surface interactions at small scales, offering methodological insights relevant to nanoplastic removal studies (Al-Abboodi et al., 2011; Alhasan et al., 2013). Together, these strands frame an integrated context in which efficient, regenerable adsorbents for nanoplastic remediation are urgently needed.

Building on the aforementioned background, the present work develops a date palm frond biochar activated by microwave heating and NaOH modification, and presents a magnetically retrievable analogue via Fe_3O_4 deposition. By coupling waste valorization with energy-lean activation and facile magnetic recovery and situating the results within a broader sustainability and public-health agenda (Benouis et al., 2022; Aziz et al., 2024; Rashid et al., 2024). This study seeks to develop practical materials to mitigate nanoplastics in complex aqueous matrices. This work aims to assess the efficacy of microwave-activated palm frond biochar for eliminating PVC nanoparticles from aqueous solutions, identify the optimal activation conditions, and enhance understanding of adsorption mechanisms through physical and chemical analyses. By characterizing the activated biochar using techniques such as FTIR, FESEM, and XRD and assessing its ability to remove nanoplastic particles, this research provides a comprehensive methodology and identifies optimal parameters, thereby facilitating extensive applications in aquatic pollution control.

Materials and Methods

Chemicals and instruments: The principal equipment includes a Fourier Transform Infrared Spectrometer (FTIR) (Shimadzu, Japan), a Field-Emission Scanning Electron Microscope (FESEM) (UPRA55 VP, Japan), an X-ray Diffractometer (XRD) (Haoyuan, China), a microwave, and a furnace. Key reagents were hydrochloric acid (HCl) (Scharlau/Riedel), sodium hydroxide (Carlo Reagent/Riedel), and acetone. Distilled water and local palm fronds were used as the primary material.

Biochar production and microwave activation: Fresh palm fronds (approximately 4 kg) were collected, thoroughly washed, and sun-dried for 30 days. Pyrolysis was performed in a furnace at 700℃ for four hours under a nitrogen atmosphere. The resulting biochar was cooled, repeatedly washed with distilled water, and then dried at 70°C in an oven. Biochar was chemically activated with varying NaOH concentrations and water under different microwave conditions. Ten grams of biochar were dispersed in 1 L NaOH at 0.5, 2.0, or 4.0 M, then microwave-irradiated under the corresponding settings: 500 W for 4.5 min (0.5 M), 800 W for 3.5 min (2.0 M), and 800 W for 5 min (4.0 M). The resulting slurries were filtered through 0.45 μm membranes, rinsed with distilled water, oven-dried, acid-washed with HCl under magnetic stirring for 15 min, rinsed with acetone for 15 min, and finally dried at 160°C for 24 h. The activated materials were then analyzed by FTIR.

Water activation: Ten grams of biochar were added to 1 L of water, and the biochar was activated in a microwave at different time intervals and power levels: 12 minutes at 1000 W, 12 minutes at 800 W, 20 minutes at 1000 W, and 20 minutes at 800 W. The sample was then washed with acetone for 15 minutes using a magnetic stirrer. Subsequently, it was filtered through filter paper and then placed in the oven for 24 hours. The activated biochar was scanned with FTIR, FESEM, and XRD at the College of Pharmacy, University of Kufa, to analyze its functional groups, surface morphology, and crystal structure.

Adsorption experiment: The adsorption experiments were conducted in a batch mode. Removal efficiency (RE) of PVC nanoplastics was calculated based on the concentration of contaminants in the solution before (C_0) and after (Ce) treatment. This equation expresses the percentage of contaminant removed from the

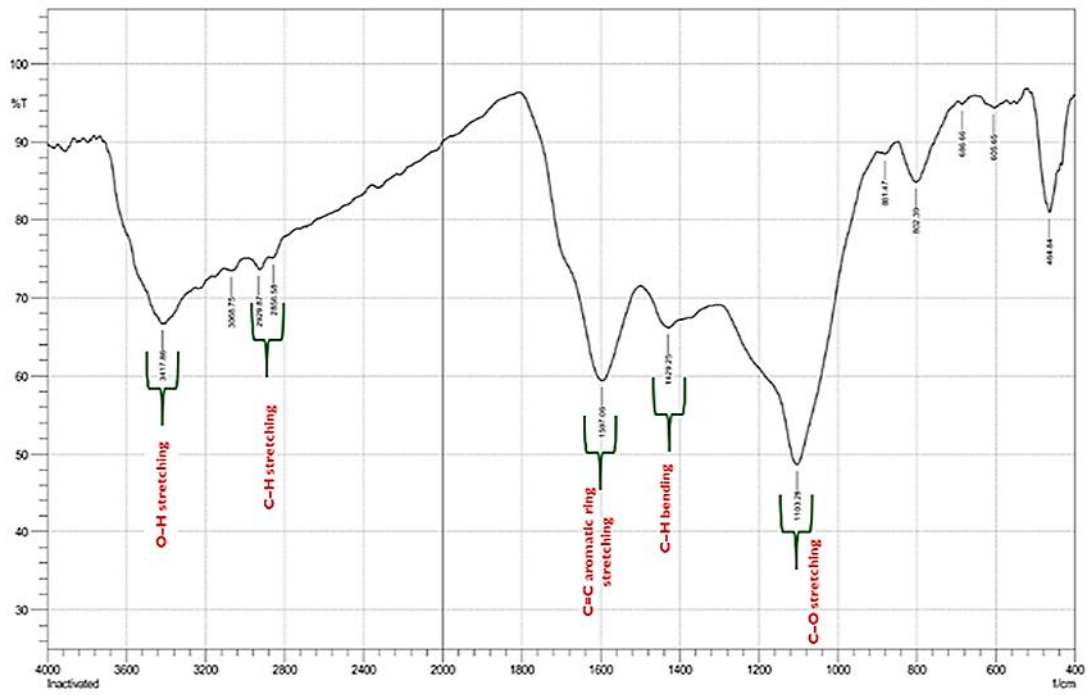

Figure 1. FTIR analysis of inactivated palm frond biochar (BC).

solution (Shakoor et al., 2020), which is calculated as: RE (%) = $[(C_0 - C_e) / C_0] \times 100$, where RE (%) is the percentage removal, C_0 is the initial concentration of the contaminant in the solution before adsorption, and C_e is the final concentration of the contaminant in the solution after adsorption, which means when equilibrium concentration is reached. All adsorption experiments were performed in triplicate to ensure data reliability. The final results presented in the discussion sections are the mean values of the replicates.

Results and Discussions

The FTIR spectrum of inactivated biochar is shown in Figure 1. The principal characteristic in this spectrum is the O-H stretching peak, which is located at approximately 3417 cm^{-1}. This broad peak indicates the presence of hydroxyl (-OH) groups, a common feature of materials containing water, alcohols, or phenols. The C-H stretching peak is situated at approximately 2929 cm^{-1}. This peak indicates the presence of alkyl C-H bonds, which are an essential part of the carbon skeleton of the material. The C=C aromatic ring stretching peak is approximately 1597 cm^{-1}. This peak indicates the presence of unsaturated aromatic rings. The C-H bending peak is situated at approximately 1429 cm^{-1}. This peak indicates the existence of C-H bonds in the carbon skeleton. The C-O stretching peak at approximately 1103 cm^{-1} suggests the existence of C-O bonds, which could be linked to alcohol, ether, or phenol groups. It can be concluded that non-activated biochar contains hydroxyl groups, alkyl bonds, and aromatic rings.

Figure 2 shows the FTIR spectrum of microwave-activated biochar. The most notable feature in this spectrum is the O-H bond peak at approximately 3366 cm^{-1}, which is distinct and indicates the presence of hydroxyl (-OH) groups. The C=O bond peak at approximately 1703 cm^{-1} is diagnostic of carbonyl groups (C=O), which are found in carboxylic acids, esters, ketones, and aldehydes. The C-O-C peak at roughly 1065 cm^{-1} indicates the ether C-O-C bonds. The C-O peaks at approximately 877 cm^{-1} and 690 cm^{-1} indicate the existence of C-O bonds, which may be associated with different compounds. It also shows a strong, significant peak at approximately 1703 cm^{-1}, corresponding to the C=O stretching vibration, in contrast to Figure 1. This indicates that microwave activation of biochar has led to surface oxidation and the formation of new carbonyl or carboxyl groups.

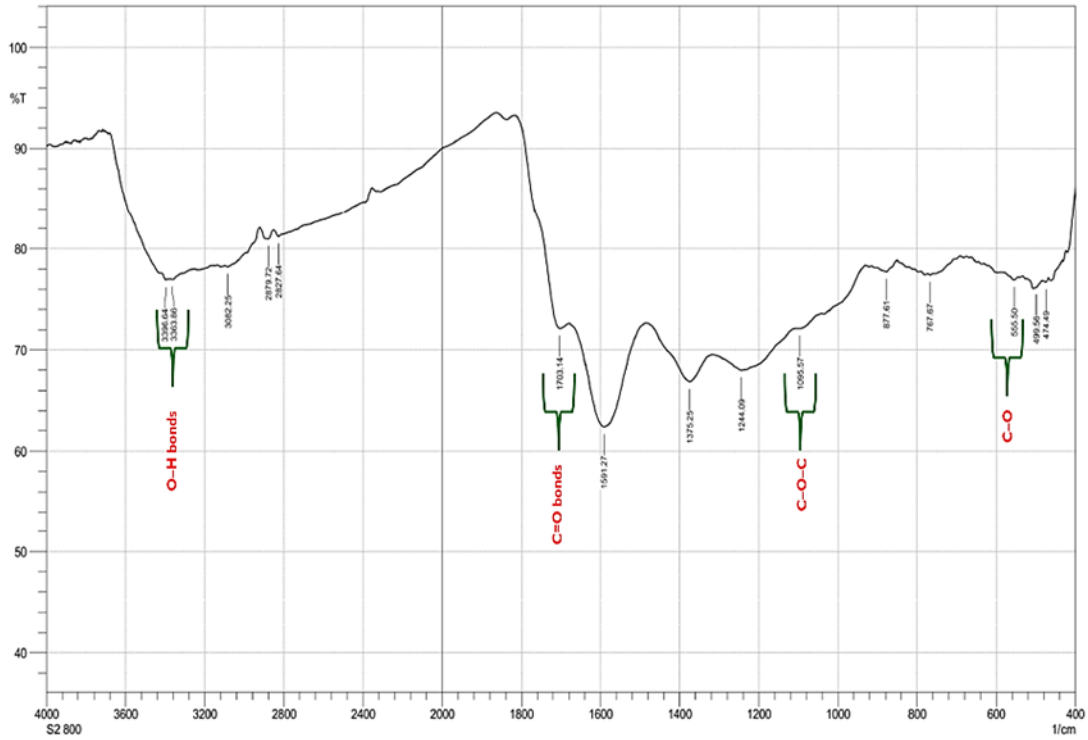

Figure 2. FTIR analysis of microwave -activated biochar (MBC) (20 min, 800 watts).

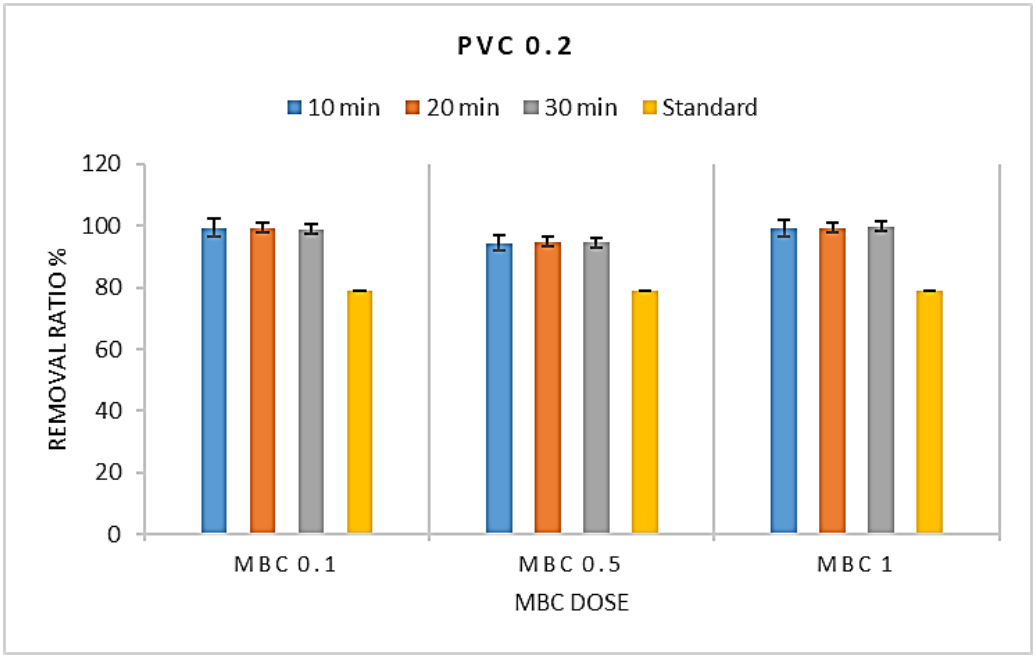

Figure 3. Effect of magnetic biochar (MBC) doses (0.1, 0.5, and 1 g) and contact time (10, 20, and 30 minutes) on the removal efficiency of PVC nanoplastics at 0.2 ppm concentration.

The C-O-C ether bonds also indicate a change in the chemical composition of the material (Yusuf, 2023). These new surface functional groups, particularly the carbonyl (C=O) and the potential carboxyl (COOH) groups, are highly ionizable in aqueous solutions (Ali et al., 2022; Banoon and Ghasemian, 2022). Deprotonation of these acidic groups significantly increases the negative charge density on the biochar surface. This enhanced negative charge is critical for promoting the primary

electrostatic interaction mechanism, thereby enabling effective attraction and capture of PVC nanoplastics in water (Wang et al., 2025). This chemical modification is therefore the fundamental reason for the highly efficient removal observed in the adsorption experiments.

The removal efficiency of nanoparticles from PVC at a concentration of 0.2 ppm using magnetic biochar (MBC) is shown in Figure 3. The results demonstrate that the biochar was highly effective in removing these particles. The removal efficiency was very high under all experimental conditions, ranging from 94 to 100%. When the biochar concentration was high (MBC 1), the removal efficiency was 100% at all time points (10, 20, and 30 minutes). This indicates that sufficient biochar was present to provide adequate adsorption sites to trap all nanoparticles. When the biochar concentration was lowered (MBC 0.5 and MBC 0.1), the removal efficiency remained very high, never falling below 94%. These findings indicate that the modified biochar is effective even at low doses. This outstanding performance is ascribed to the distinctive characteristics of the biochar.

These results also indicate that contact duration (10, 20, and 30 minutes) had no significant influence on removal efficiency under the specified conditions (Fig. 3). Maximum elimination was attained rapidly (within 10 minutes) at all biochar concentrations. This indicates that the adsorption process was rapid and efficient, which is advantageous for water treatment applications. The rapidity is frequently attributed to the extensive surface area and elevated porosity of biochar, as well as to robust interactions between its surface and nanoparticles. The process of nanoparticle removal depends on multiple critical factors, including physical adsorption, hydrophobic interactions, and electrostatic attraction. Biochar exhibits significant porosity and a large surface area, providing numerous adsorption sites for nanoparticles (Han et al., 2024). These particles can be physically confined within pores or on surfaces. These interactions constitute a primary mechanism of removal. The FTIR analysis confirmed the formation of new carbonyl groups (C=O) at 1703 cm^{-1}, which readily dissociate in the aqueous solution, significantly increasing the negative charge density on the biochar surface. This microwave-activated chemical modification significantly enhances the electrostatic attraction between the MBC and PVC nanoplastics, thereby accounting for the high adsorption efficiency of up to 100% in aquatic environments. Due to its hydrophobicity, PVC tends to adhere to hydrophobic surfaces, such as biochar (Nosratabad et al., 2024). Biochar also functions as a flocculant, aggregating nanoparticles into larger clusters, thereby enhancing their clearance.

Figure 4 shows that the removal efficiency of nanoparticles from PVC plastic ranged between 89 and 97% at a concentration of 0.6 ppm. Compared with the data in Figure 3 (0.2 ppm), where the removal efficiency reached 100%, the removal efficiency decreased as the nanoparticle concentration in the solution increased. As the concentration of the contaminant (nanoparticles) increases, the number of available adsorption sites on the biochar surface becomes more crowded, leading to faster saturation. As a result, the same amount of biochar may not remove the same percentage of contaminants. In contrast to the previous concentration (0.2 ppm), increasing contact time has a positive effect on removal efficiencyFigure 3, increasing contact time has a positive effect on removal efficiency (Fig. 4). At all biochar concentrations (MBC 1, MBC 0.5, MBC 0.1), the removal efficiency of nanoparticles after 30 minutes was higher than after 10 minutes. This indicates that the adsorption process has not reached equilibrium after 10 minutes and that a longer time is required for the nanoparticles to diffuse into the biochar's internal sites and form stable bonds (Liu et al., 2022). Physical adsorption remains key, with PVC nanoparticles adsorbed onto the biochar surface due to its high porosity and large surface area (Leng et al., 2021). As particle concentration increases, competition for adsorption sites intensifies, resulting in the observed reduction in relative removal efficiency. The realine at longer contact times (up to 30 minutes) indicates that intraparticle diffusion within the internal pore structure becomes the rate-

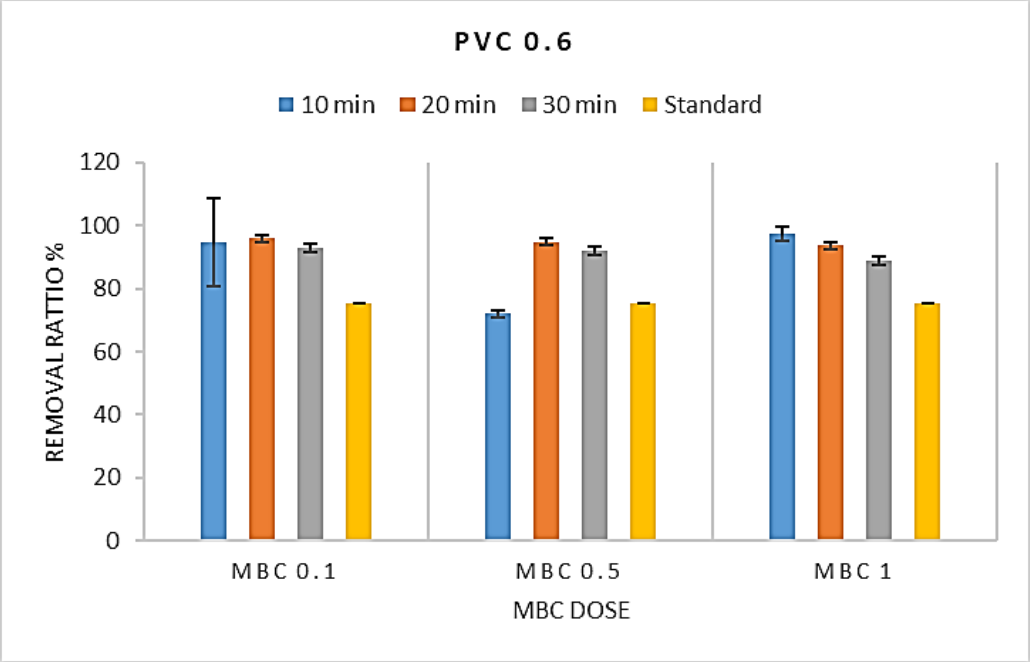

Figure 4. Effect of magnetic biochar (MBC) doses (0.1,0.5, and 1 g) and contact time (10, 20, and 30 minutes) on the removal efficiency of PVC nanoplastics at 0.6 ppm concentration.

limiting step at this higher concentration.

Electrostatic interactions are crucial, as the FTIR analysis confirmed the formation of surface functional groups and a significant negative surface charge. These charges critically enhance the electrostatic attraction and trapping of PVC nanoplastics (Zhao et al., 2025). Hydrophobic interactions also occur, as both PVC and the carbon structure of biochar are water-repellent, promoting strong PVC-MBC bonding and contributing to sustained high removal efficiency (Trivedi et al., 2025). Despite a slight decrease in efficiency due to higher nanoplastic loading, the MBC still achieved a remarkable 97% removal at 0.6 ppm. This performance highlights its superiority over many conventional adsorbents. Several studies on magnetic biochar for nanoplastic removal reported equilibrium capacities that were surpassed by the high percentage removal achieved here under the optimal conditions, confirming the material's strong potential for aquatic remediation even when challenged with higher contaminant levels.

The removal efficiency of PVC nanoparticles at a high concentration (1 ppm) using modified biochar (MBC) is shown in Figure 5. The results show that removal efficiency remains high overall but varies significantly relative to lower concentrations (0.2 and 0.6 ppm). At 1 ppm, removal efficiency decreased significantly in some cases compared to previous results. Increasing contact time improves removal efficiency, particularly at lower biochar doses. This indicates that at this high concentration (1 ppm), the adsorption process did not reach rapid equilibrium. Instead, the rate-limiting step shifted to intraparticle diffusion, necessitating more time for the PVC nanoplastic to overcome the concentration gradient and fully diffuse into the internal, porous sites of the biochar (confirmed by FESEM), thus allowing for the formation of stable bonds. The findings revealed that the abundance of active sites on the biochar surface enables rapid and efficient adsorption even at high contaminant concentrations (Jagadeesh and Sundaram, 2023). Despite the competitive stress caused by the high PVC concentration (1 ppm), the modified biochar demonstrated exceptional robustness, achieving 99% removal at the highest dose (MBC 1). This robust performance is highly significant for practical applications, as it proves that microwave-activated palm frond biochar is effective even under high-contamination conditions. This quantitative efficiency places the material among the top-performing adsorbents for nanoplastic remediation in water, validating its potential for large-

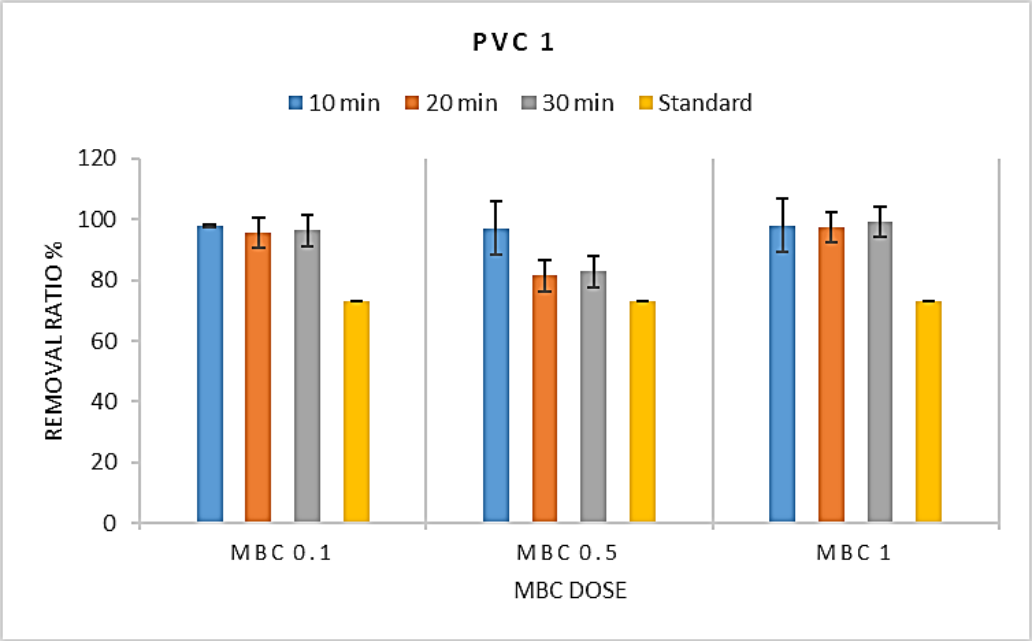

Figure 5. Effect of magnetic biochar (MBC) doses (0.1, 0.5, and 1 g) and contact time (10, 20, and 30 minutes) on the removal efficiency of PVC nanoplastics at 1 ppm concentration.

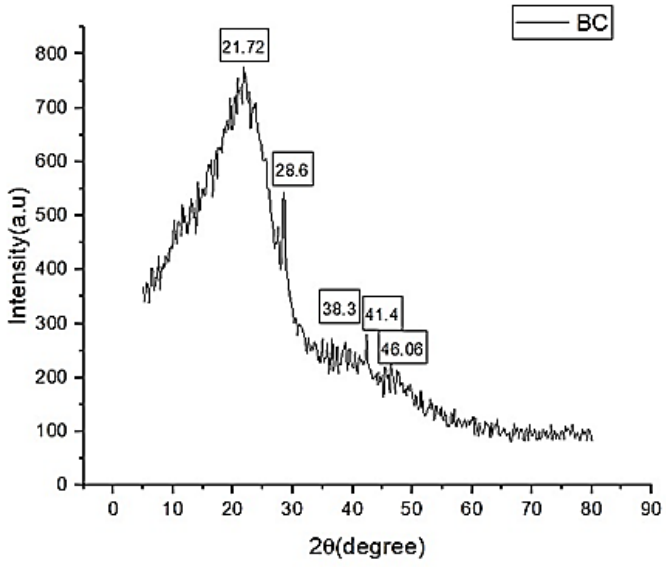

Figure 6. XRD result of biochar.

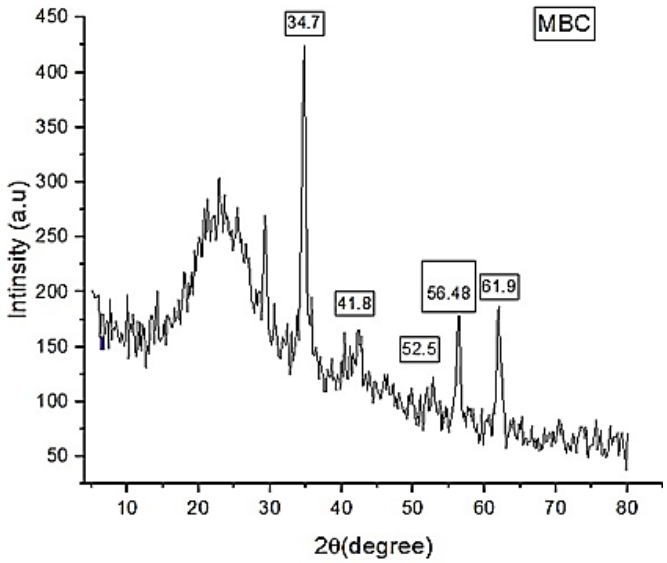

Figure 7. XRD result of Magnetic biochar.

scale application in aquatic pollution control.

The XRD spectrum of biochar (BC), which is amorphous, is shown in Figure 6. The BC XRD spectrum shows a broad, diffuse peak centered at approximately 21.72°(2θ). Smaller, less defined peaks are also present at 28.6°, 38.3°, 41.4°, and 46.06°. The presence of a broad peak at 21.72° is a characteristic sign of an amorphous biochar structure. This means that the material lacks a regular, long-range crystalline structure. This structure indicates that biochar is composed of irregular, non-orderly stacked carbon layers. This peak is known as the characteristic peak of the (002) plane of unordered graphitic carbon. Other small peaks may be due to trace amounts of crystalline impurities or poorly ordered carbon regions.

Figure 7 shows the XRD results for magnetic biochar (MBC), indicating sharp, well-defined peaks

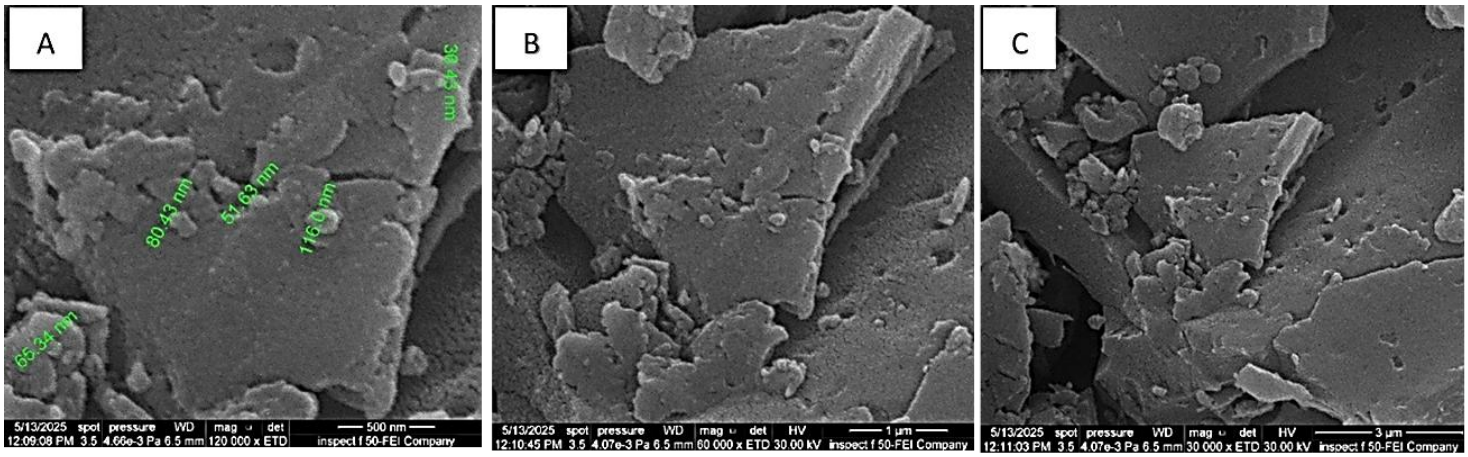

Figure 8. FESEM images for activated biochar (palm fronds). (A) activated biochar (scale bar = 500 nm), (B) activated biochar (scale bar = 1 µm), and (C) activated biochar (scale bar = 3 µm).

at 34.7°, 41.8°, 52.5°, 56.48°, and 61.9° (2θ). The peak at 34.7° is the sharpest and most intense. The appearance of these sharp, distinct peaks confirms that the magnetic biochar has a crystalline structure. The locations of these peaks correspond to the characteristic diffraction peaks of a magnetic material, most likely magnetite (Fe_3O_4) or another iron oxide phase, such as maghemite (γ-Fe2O3). The prominent peak at 34.7° is a definitive diffraction peak of magnetite, indicating magnetite formation with high crystallinity.

XRD analysis provides essential insights into the biochar magnetization process, showing a transition from an amorphous structure (Fig. 6) to a crystalline structure (Fig. 7). This confirms that magnetization has introduced a new, highly ordered crystalline phase into the biochar. The sharp peaks in the MBC spectrum are direct evidence of the successful formation of a crystalline magnetic material, such as magnetite (Fe_3O_4). This is the primary objective of the magnetization process, leading to the desired magnetic properties. The presence of a magnetic crystalline phase imparts magnetic properties to magnetic biochar, which are essential for the separation and recovery of treated wastewater using a magnetic field. In contrast, unmodified biochar (BC) has no magnetic properties. Several studies indicate that biochar produced at low temperatures (usually below 700°C) exhibits a non-crystalline structure with a large peak around 20-30° (2θ) (Zhang et al., 2019). Numerous investigations have shown that the sharp peaks observed in the XRD spectrum of magnetic biochar are characteristic of magnetic iron oxides (Zhang et al., 2024). This indicates that the appearance of these peaks is a key indicator of the success of the modification process.

Based on the field-emission scanning electron microscope (FESEM) images (Fig. 8), the activated biochar exhibits a highly porous surface and an irregular structure. The photos, taken at different magnifications, show a rough texture with numerous pores and cavities of varying sizes. This texture is a key characteristic of an effective adsorbent. The FESEM images provide a visual representation of the microscopic structure of biochar, which is crucial for understanding its performance in adsorption applications. Images (Fig. 8A, B, C) show that the activated biochar is not a solid, smooth mass, but rather a complex, heterogeneous material. It has a rough texture with visible cracks, cavities, and pores. This irregular shape is a direct result of high-temperature pyrolysis and activation processes, which remove volatiles and leave a porous carbon structure. The presence of numerous pores is associated with a large surface area. Adsorption is a surface phenomenon; therefore, a larger surface area provides more active sites for nanoparticles to adhere to. The visible pores and channels facilitate the transport of contaminants into the biochar particles, enhancing the overall removal efficiency.

The observed microstructure supports the proposed adsorption mechanisms. The pores act as physical

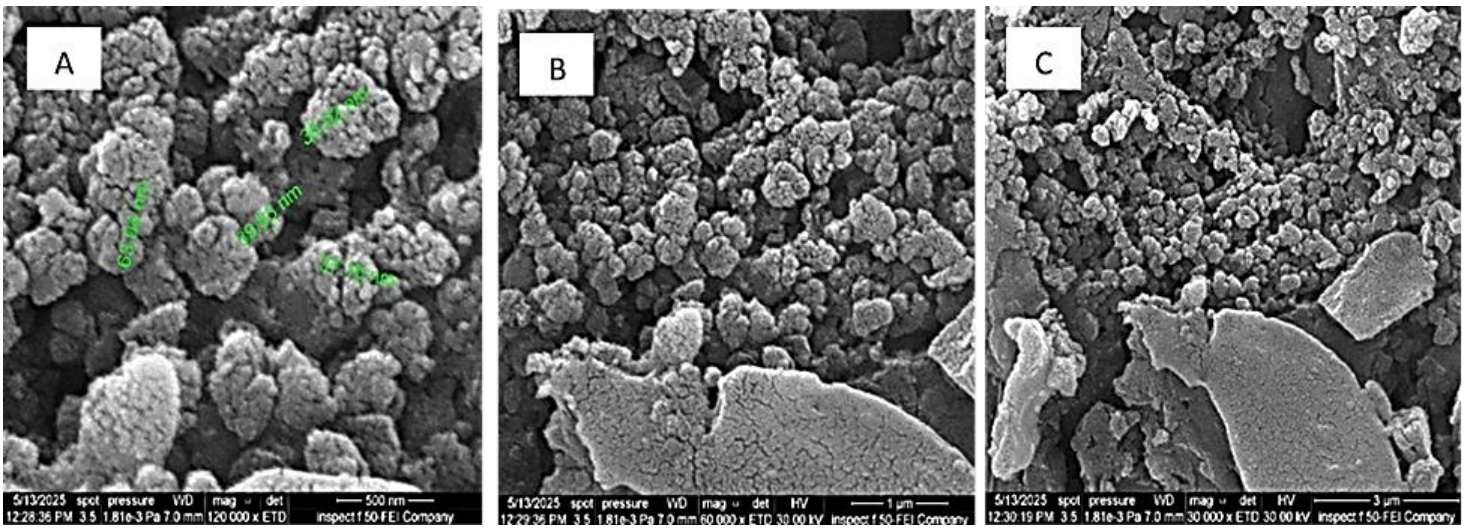

Figure 9. FESEM images for magnetized biochar (activated biochar powder + Fe3O4). (A) magnetized biochar (scale bar = 500 nm), (B) magnetized biochar (scale bar =1 μm), and (C) magnetized biochar (scale bar = 3 μm)

traps for PVC nanoparticles, enabling their adsorption and retention. Physical adsorption is a key mechanism for contaminant removal in biochar. Additionally, the irregular, rough surface increases the chances of physical contact between the biochar and the nanoparticles, promoting strong binding. The images at different magnifications (from 3 μm to 500 nm) show the presence of particles of various sizes, including some clusters in the nanoscale range. The visible pores on the surface also vary in size, ranging from micropores to macropores, consistent with the heterogeneous pore-size distribution in biochar. This diverse porous structure is ideal for retaining contaminants of various sizes. Previous studies, consistent with our findings, have confirmed that the thermal decomposition and activation of biomass, particularly from palm fronds, yield highly porous structures. FESEM images of palm biochar have shown similarities, highlighting well-defined pores and channels that contribute to increased surface area (Torrarit et al., 2025). The morphological characteristics in FESEM images, namely, high porosity and large surface area, are the primary reasons for biochar's effectiveness in removing organic and inorganic pollutants from water (Elbehiry et al., 2022).

Figure 9 shows the successful magnetization of biochar and the resulting enhancement of magnetic properties. The images clearly show spherical, agglomerated particles on the rough, porous surface of the biochar. These particles are likely magnetite (Fe_3O_4) nanoparticles deposited on the biochar surface. The sizes of these particles range from a few tens to hundreds of nanometers, as indicated by the scale in the images. The images show a close interaction between the magnetite NPs (Fe_3O_4) and the main body of the biochar. Rather than being isolated, the magnetite particles are dispersed and adhered to the porous surface of the biochar. This adhesion is crucial because it prevents the magnetic particles from separating during application and ensures that the magnetized biochar remains a single, recoverable unit. The presence of magnetite nanoparticles imparts magnetic properties to the biochar. This property enables the material to be readily separated from the solution after water treatment, thereby facilitating its reuse. Although FESEM images do not directly capture the adsorption process, the presence of the magnetic material on the biochar's porous surface does not significantly reduce its surface area. It may even enhance certain adsorption mechanisms by providing additional adsorption sites. The images clearly demonstrate that the biochar still retains its basic porous structure. These FESEM results align with previous studies that show the structural morphology of magnetized biochar. FESEM images of magnetite particles coated with biochar showed spherical magnetite particles adhering to the biochar's rough

surface, which is consistent with the results of Liu et al. (2020). Other studies indicate that magnetizing biochar with magnetic particles does not significantly alter its surface area but instead enables magnetic separation, making it more practical and cost-effective for large-scale water treatment applications (Baharudin et al., 2022).

Conclusion

Microwave-activated magnetic biochar (MBC) represents a promising, cost-effective, and highly effective solution for aquatic pollution control, particularly in addressing PVC nanoplastic contamination. The results of the current work confirmed that microwave activation is a simple and efficient method, with optimal conditions (800 W for 20 minutes), yielding a material that achieved exceptional removal efficiencies of up to 100% at 0.2 ppm and 99% at 1 ppm. This superior performance is attributable to the successful formation of a highly porous structure (as evidenced by FESEM) and a substantial increase in electrostatic binding sites (as evidenced by the formation of carbonyl (C=O) groups via FTIR). The magnetic property facilitates efficient and cost-effective recovery from aqueous solutions, establishing MBC as a sustainable alternative.

References

Al-Abboodi A., Tjeung R., Doran P., Yeo L., Friend J., Chan P. (2011). Microfluidic chip containing porous gradient for chemotaxis study. Smart Nano-Micro Materials and Devices, 8204: 219-224.

Alhasan L., Qi A., Al-Aboodi A., Rezk A., Shilton R.R., Chan P.P., ... Yeo L. (2013). Surface acoustic streaming in microfluidic system for rapid multicellular tumor spheroids generation. Micro/Nano Materials, Devices, and Systems, 8923: 828-831.

Ali Z.H., Al-Saady M.A.A.J., Aldujaili N.H., Rabeea Banoon S., Abboodi A. (2022). Evaluation of the antibacterial inhibitory activity of chitosan nanoparticles biosynthesized by *Streptococcus thermophilus*. Journal of Nanostructures, 12(3): 675-685.

Al-Saady A.J., Aldujaili N.H., Banoon S.R., Al-Abboodi A. (2022). Antimicrobial properties of nanoparticles in biofilms. Revis Bionatura, 7(4): 71.

Aziz Z.S., Jazza S.H., Dageem H.N., Banoon S.R., Balboul B.A., Abdelzaher M.A. (2024). Bacterial biodegradation of oil-contaminated soil for pollutant abatement contributing to achieve sustainable development goals: A comprehensive review. Results in Engineering, 22: 102083.

Baharudin N.I.S., Noor N.M., Abdullah E.C., Othman R., Mujawar M.N. (2022). Magnetically modified sugarcane bagasse biochar as cadmium removal agent in water. IIUM Engineering Journal, 23(1): 294-309.

Banoon S.R., Ghasemian A. (2022). The characters of graphene oxide nanoparticles and doxorubicin against HCT-116 colorectal cancer cells in vitro. Journal Of Gastrointestinal Cancer, 53(2): 410-414.

Bashir I., Lone F.A., Bhat R.A., Mir S.A., Dar Z.A., Dar, S.A. (2020). Concerns and threats of contamination on aquatic ecosystems. In: Bioremediation and biotechnology: sustainable approaches to pollution degradation. pp. 1-26.

Benouis K., Khane Y., Ahmed T., Albukhaty S., Banoon S.R. (2022). Valorization of diatomaceous earth as a sustainable eco-coagulant for wastewater treatment: optimization by response surface methodology. Egyptian Journal of Chemistry, 65(9): 777-788.

Elbehiry F., Darweesh M., Al-Anany F.S., Khalifa A.M., Almashad A.A., El-Ramady H., ... Elbasiouny H. (2022). Using biochar and nanobiochar of water hyacinth and black tea waste in metals removal from aqueous solutions. Sustainability, 14(16): 10118.

Fadhil A.A., Mohammed S.J., Al-Abboodi A. (2023). Morphological responses of plants to air pollutants: A comparative study on leaf changes in five species. Iranian Journal of Ichthyology, 10: 286-293.

Fadhil A.A., Swaid S.Y., Mohammed S.J., Al-Abboodi A. (2024). Impact of salinity on tomato seedling development: A comparative study of germination and growth dynamics in different cultivars. Journal of Chemical Health Risks, 14(1): 183-190.

Han M., Liu Z., Huang S., Zhang H., Yang H., Liu Y., ... Zeng Y. (2024). Application of Biochar-Based Materials for Effective Pollutant Removal in Wastewater Treatment. Nanomaterials, 14(23): 1933.

He D., Luo Y., Zhu B. (2024). Feedstock and pyrolysis temperature influence biochar properties and its interactions with soil substances: Insights from a DFT calculation. Science of the Total Environment, 922: 171259.

Jagadeesh N., Sundaram B. (2023). Adsorption of pollutants from wastewater by biochar: a review. Journal of Hazardous Materials Advances, 9: 100226.

Lalrinfela P., Vanlalsangi R., Lalrinzuali K., Babu P.J. (2024). Microplastics: Their effects on the environment, human health, and plant ecosystems. Environmental Pollution and Management, 1: 248-259.

Leng L., Xiong Q., Yang L., Li H., Zhou Y., Zhang W., ... Huang H. (2021). An overview on engineering the surface area and porosity of biochar. Science of the Total Environment, 763: 144204.

Liu Y., Huang J., Xu H., Zhang Y., Hu T., Chen W., ... Jiang G. (2020). A magnetic macro-porous biochar sphere as vehicle for the activation and removal of heavy metals from contaminated agricultural soil. Chemical Engineering Journal, 390: 124638.

Liu Y., Ma J., Gao J., Chen X., Ouyang X., Weng L., ... Li Y. (2022). Stability and interaction of biochar and iron mineral nanoparticles: effect of pH, ionic strength, and dissolved organic matter. Biochar, 4(1): 47.

Nosratabad N.A., Yan Q., Cai Z., Wan C. (2024). Exploring nanomaterial-modified biochar for environmental remediation applications. Heliyon, 10(18).

Paramasivan B. (2022). Microwave assisted carbonization and activation of biochar for energy-environment nexus: A review. Chemosphere, 286: 131631.

Rashid M.K., Salman I.R., Obaid A.L., Hassan S.A.D.H., Al-Musawi M.R., Al-Saady M. (2024). Application of machine learning in predicting sources of water pollution in the Euphrates and Tigris rivers in Iraq. International Journal of Aquatic Biology, 12(6): 581-589.

Sahira K., Al-Abboodi A.K. (2023). Parasitological Contamination of Raw Vegetables collected from selected Local Markets in Maysan Province, South of Iraq. Nigerian Journal of Parasitology, 44(2).

Salman I.R., Rasheed A.A., Hassan S.A.D.H., Hussein R.A., Al-Saady M. (2025). Automated aquatic biodiversity monitoring using deep learning on the Tigris River: Species identification and ecosystem assessment. International Journal of Aquatic Biology, 13(1): 30-40.

Shakoor M.B., Ali S., Rizwan M., Abbas F., Bibi I., Riaz M., ... Rinklebe J. (2020). A review of biochar-based sorbents for separation of heavy metals from water. International Journal of Phytoremediation, 22(2): 111-126.

Singh N., Khandelwal N., Ganie Z.A., Tiwari E., Darbha G.K. (2021). Eco-friendly magnetic biochar: An effective trap for nanoplastics of varying surface functionality and size in the aqueous environment. Chemical Engineering Journal, 418: 129405.

Tan X., Liu Y., Zeng G., Wang X., Hu X., Gu Y., Yang Z. (2015). Application of biochar for the removal of pollutants from aqueous solutions. Chemosphere, 125: 70-85.

Torrarit P., Poompradub S., Mohammadifar M., Pattananuwat P., Jayaraman T., Jeong Y., ... Kasemchainan J. (2025). Highly porous activated carbon from betel palm shells as the prospective electrode for high-performance supercapacitors. Materials Science for Energy Technologies, 8: 143-153.

Trivedi Y., Sharma M., Mishra R.K., Sharma A., Joshi J., Gupta A.B., ... Vuppaladadiyamd A.K. (2025). Biochar potential for pollutant removal during wastewater treatment: A comprehensive review of separation mechanisms, technological integration, and process analysis. Desalination, 118509.

Wang Y., Wu M., Hao Y., Li H., Mo C. (2025). Surfactant-mediated transport of polyvinyl chloride nanoplastics in porous media: Influence of natural organic matter, natural inorganic ligands and electrolytes. Journal of Contaminant Hydrology, 104597.

Yi S., Sun Y., Hu X., Xu H., Gao B., Wu J. (2018). Porous nano-cerium oxide wood chip biochar composites for aqueous levofloxacin removal and sorption mechanism insights. Environmental Science and Pollution Research, 25(26): 25629-25637.

Yusuf M.O. (2023). Bond characterization in cementitious material binders using Fourier-transform infrared spectroscopy. Applied Sciences, 13(5): 3353.

Zhang B., Zhou S., Zhou L., Wen J., Yuan Y. (2019). Pyrolysis temperature-dependent electron transfer capacities of dissolved organic matters derived from wheat straw biochar. Science of the Total Environment, 696: 133895.

Zhang M., Song G., Gelardi D.L., Huang L., Khan E., Mašek O., ... Ok Y.S. (2020). Evaluating biochar and its modifications for the removal of ammonium, nitrate, and phosphate in water. Water Research, 186: 116303.

Zhang W.W., Ma X., Yang Z., Ren Z.L., Yang X., Zhao Z.W. (2024). Polyrhodanine-functionalized magnetic-activated Carbon for efficient removal of lead ions and Malachite Green from Wastewater. Nano, 19(02): 2450005.

Zhao X., Liao Z., Zhao Q., Yang M., Li D., Zhang K., ... Zheng B. (2025). A low-cost magnetic biochar manufactured solely from solid wastes by one-step pyrolysis for removal of tetracycline. Scientific Reports, 15(1): 30035.